SUPPLEMENTAL DATA

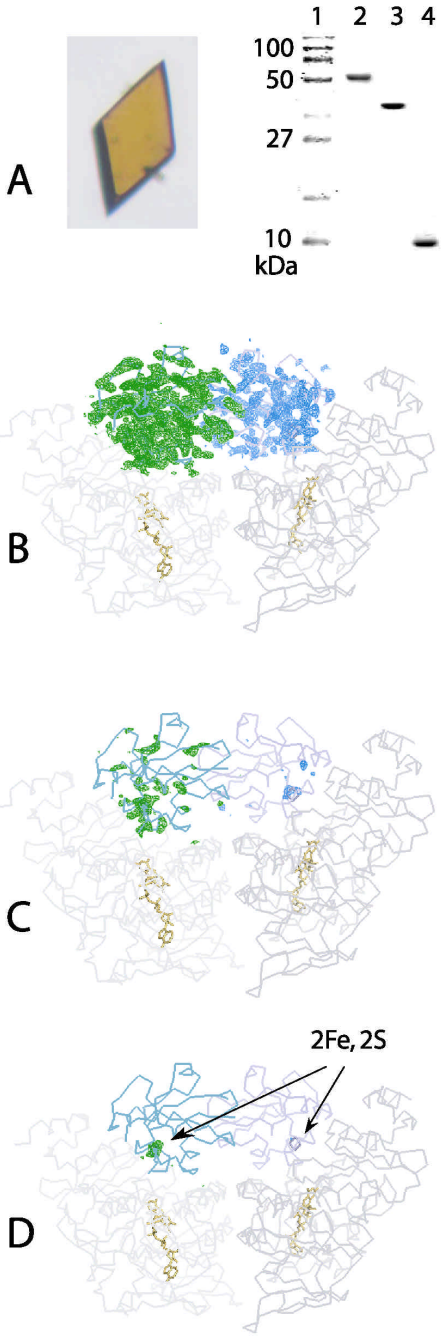

Figure 1S. (A) A crystal of the covalent Pdr-Pdx complex and a 10-15% SDS-PAGE gradient gel, where lane 1 - Precision Plus protein standards (Bio-Rad), lane 2 - dissolved crystals of the covalent Pdr-Pdx complex, lanes 3 and 4 - intact Pdr and Pdx, respectively. (B-D), Simulated annealing omit maps for two Pdx molecules contoured at 1.0, 2.0 and 3.0 σ, respectively. Electron density around Pdx in complexes 1 and 2 is shown in green and blue, respectively. Positions of the metal clusters are indicated by arrows.

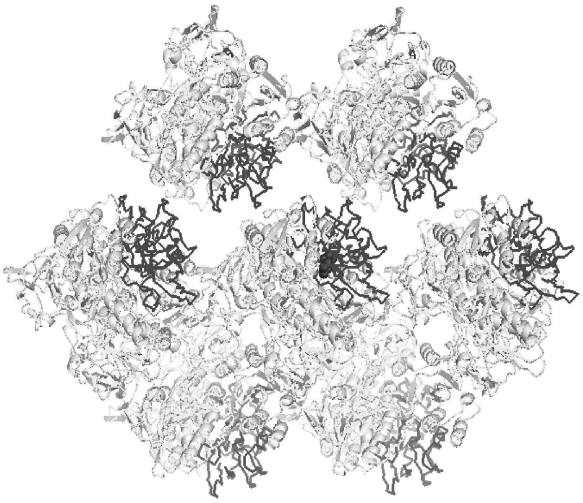

Figure 2S. Packing of the Pdr-Pdx complex in the crystal lattice. Pdr and Pdx are in gray and black, respectively. Pdx is fully exposed into the solvent channel and forms contacts only with the attached Pdr.

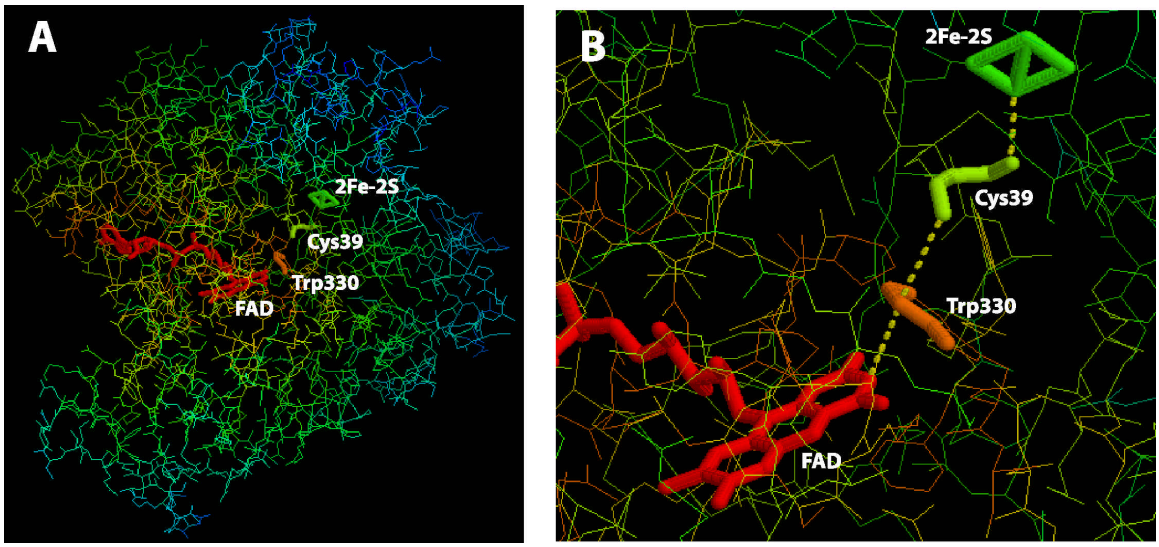

Figure 3S. (A), Electronic coupling between the flavin and metal centers in the crosslinked Pdr-Pdx complex calculated using the program HARLEM (1) with the default settings and the entire FAD and [2Fe-2S] moieties defined as electron donor and acceptor groups, respectively. Residues are colored according to the strength of the electronic coupling (red >> blue). (B), A magnified view at the active site with a predicted electron transfer pathway. Details on how electronic coupling and pathways between the electron donor and acceptor groups are calculated can be found at:
http://www.kurnikov.org/harlem_manual/html/page_et_calc.html

Table 1S. *Electronic coupling, pathway and electron transfer rate for the crosslinked Pdr-Pdx complex calculated with the program HARLEM (1).*

For the analysis, the entire FAD and [2Fe-2S] moieties were defined as electron transfer donor and acceptor, respectively, and the default HARLEM settings were used.

FAD-[2Fe-2S] edge-to-edge distance (Å)	12.0
Electronic coupling (H_{AB})[a]	5.2×10^{-5}
Atom packing density (ρ)[b]	0.61
Average decay exponent (β) ($Å^{-1}$)[c]	1.63
Electron pathway[d]	FAD(N3)-Trp330^{Pdr}-Cys39^{Pdx}-Fe1
Maximum electron transfer rate (s^{-1})[e]	2.7×10^{5}

[a] H_{AB} is the dimensionless electronic tunneling coupling matrix element between donor and acceptor (2).
[b] Volume fraction between redox cofactors within the united van der Waals radius of intervening atoms (3).
[c] β is a parameter in the term $e^{-\beta R}$ that represents the exponential fall-off of the electronic tunneling rate with distance, R.
[d] Atoms and residues selected for the best electron transfer path from FAD to the [2Fe-2S] cluster.
[e] Maximum electron transfer rate predicted for this particular electron pathway.

Molecular Dynamics Simulation

The main purpose of the molecular dynamics (MD) simulation was to check the stability of some key interactions between Pdx and Pdr found in the crystal structure. We started with a Pdr-Pdx complex derived from the crystallographic complex 1. The Amber 9.0 suite (4) was used for all calculations, and ff99 forcefield provided with the Amber 9.0 package was used for the protein. Parameters for FAD were derived with Antechamber and the Gaff forcefield (2) using the BCC charging scheme (6, 7). Charges for [2Fe-2S] were derived from a density functional calculation (Jaguar, Schrodinger, Inc.) using the 6-31g* basis set and the B3LYP functional. Fe-S bond distances and angles were based on the average values taken from the Pdx crystal structures (8, 9). To prepare the complex for molecular dynamics, the structure was stripped of all crystallographic water molecules except for 4 water molecules at the Pdr-Pdx intermolecular interface. The complex then was solvated in a periodic box of TIP3 water molecules using a 10 Å cushion, and 21 sodium ions added to retain charge neutrality. The $Lys409^{Pdr}$-$Glu72^{Pdx}$ covalent bond was not included. The final system contained a total of 45,359 atoms.

The structure was prepared by first energy minimization for 1000 cycles with all heavy atoms except water molecules fixed in position, followed by a short 10 ps MD run to allow just the water molecules to relax, and final 1000 cycles of energy minimization with all atoms allowed to move. The 15 ns run at 300 K was carried out with a 2 fs time step and coordinates saved every 10 ps. Temperature and pressure were held constant through a weak coupling with a 1 ps pressure relaxation time and Langevin dynamics using a collision frequency of 1 ps^{-1}. Periodic boundary conditions were used with a Particle Mesh Ewald implementation of the Ewald sum for the description of long-range electrostatic interactions (10). A spherical cutoff of 8.5 Å was used for nonbonded interactions. Bonds involving hydrogen atoms were constrained using SHAKE (11). Analysis of the final trajectory was carried out with Ptraj in the Amber 9.0 suite.

Since Pdr and Pdx were not covalently attached, we treated each molecule separately in the analysis of the 15 ns trajectory. As evidenced by the r.m.s.d. of backbone atoms, the trajectory for both Pdr and Pdx stabilized within 6-7 ns (Fig. 4S). The r.m.s.d. for Pdx was unusually high, leveling off at 4 Å at around 6 ns. This was due primarily to an extended section on the Pdx surface that has no regular secondary

structure (residues 58-69), whose backbone atoms moved by as much as 6.0 Å. If this segment is excluded from the r.m.s.d. calculation, the r.m.s.d. levels off near 2.6 Å (Fig. 4S).

The complex was stable over the entire 15 ns MD trajectory. For example, the closest distance between the Pdx Fe1 and Pdr FAD(N3) atoms (12.0 Å in the x-ray structure) remained at 12.75 ± 0.69Å. Another important distance is the ion pair interaction between $Arg310^{Pdr}$ and $Asp38^{Pdx}$. The distance between the Arg310(CZ) and Asp38(CD) atoms, which is 3.7Å in the crystal structure, remained quite stable at 3.98 ± 0.24 Å over the 15 ns trajectory. Although the intermolecular $Glu72^{pdx}$-$Lys409^{pdr}$ crosslink was not treated as a covalent bond, this ion pair interaction was also stable, with the distance between Glu72(CD) and Lys409(NZ) remaining at 3.67 ± 0.69Å. Overall, the MD results show that the key intermolecular interactions predicted from the previous mutagenesis results (12-15) and the present crystal structure remain intact over the entire 15 ns simulation and, hence, may be important for association/stabilization of the Pdr-Pdx electron transfer complex.

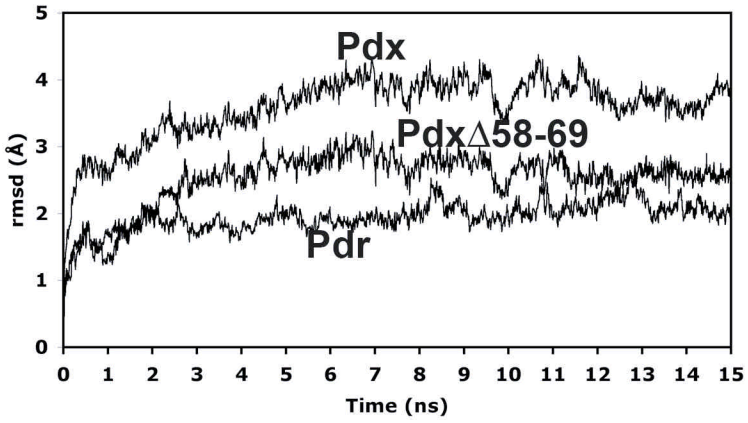

Figure 4S. Root mean square deviation (r.m.s.d.) of backbone atoms (Cα, C, N) relative to the initial starting structure. Pdx and Pdr were treated separately as noncovalently bound molecules. PdxΔ58-69 refers to Pdx with residues 58-69 excluded from the r.m.s.d. calculation.

The PYMOL file with the Pdr-Pdx complex MD simulation can be accessed at:

http://crystal.bio.uci.edu/~poulos/Public/md1to1500every20.pse

Although coordinates were saved every 10 ps over the 15 ns interval, giving a total of 1500 snapshots, only snapshots every 200 ps are included into the demonstration file to reduce its size. Residues in Pdx are numbered from 1 to 104, [2Fe-2S] is 105; residues in Pdr are numbered from 106 to 524, and FAD is 525.

REFERENCES

1. Kurnikov, I. V. (2000) *v 1.0, Department of Chemistry, University of Pittsburgh, Pittsburgh, PA*.
2. Beratan, D. N., Onuchic, J. N., Winkler, J. R., and Gray, H. B. (1992) Science **258**, 1740-1741.
3. Page, C. C., Moser, C. C., Chen, X., and Dutton, P. L. (1999) Nature **402**, 47-52.
4. Case, D. A., Cheatham, T. E., Darden, T., Gohlke, H., Luo, R., Merz, K. M., Onufriev, A., Simmerling, C., Wang, B., and Woods, R. J. (2005) *J. Comp. Chem.* **26**, 1668-1688.
5. Wang, J., Wolf, R. M., Caldwell, J. W., Kollman, P. A., and Case, D. (2004) *J. Amer. Chem. Soc.* **25**, 1157-1174.
6. Jakalian, A., Bush, B. L., Jack, D. B., and Bayly, C. I. (2000) *J. Comp. Chem.* **21**, 132-146.
7. Jakalian, A., Jack, D. B., and Bayly, C. I. (2002) *J. Comp. Chem.* **23**, 1623-1641.
8. Sevrioukova, I. F., Garcia, C., Li, H., Bhaskar, B., and Poulos, T. L. (2003) *J. Mol. Biol.* **333**, 377-392.
9. Sevrioukova, I. F. (2005) *J. Mol. Biol.* **347**, 607-621.
10. Darden, T., York, D., and Pedersen, L. (1993) *J. Chem. Phys.* **103**, 8577-8593.
11. Miyamoto, S., and Kollman, P. A. (1992) *J. Comp. Chem.* **13**, 952-962.
12. Holden, M., Mayhew, M., Bunk, D., Roitberg, A., and Vilker, V. (1997) *J. Biol. Chem.* **272**, 21720-21725.
13. Aoki, M., Ishimori, K., Morishima, I., and Wada, Y. (1998) *Inorg. Chim. Acta* **272**, 80-8816.
14. Kuznetsov, V. Y., Blair, E., Farmer, P. J., Poulos, T. L., Pifferitti, A., and Sevrioukova, I. F. (2005) *J. Biol. Chem.* **280**, 16135-16142.
15. Churbanova, I. Y., Poulos, T. L., and Sevrioukova, I. F. (2010) *Biochemistry* **49**, 58-67.